Closed-orbit theory and the photodetachment cross section of H⁻ in parallel electric and magnetic fields

Aaron D. Peters and Charles Jaffé

Department of Chemistry, West Virginia University, Morgantown, West Virginia 23506

John B. Delos

Department of Physics, College of William and Mary, Williamsburg, Virginia 23187
and JILA, University of Colorado, Boulder, Colorado 80309-0440
(Received 3 June 1996; revised manuscript received 31 January 1997)

In this paper we obtain a simple analytic formula for the photodetachment cross section of H⁻ in parallel electric and magnetic fields. The three-dimensional semiclassical approximation predicts oscillations in the spectrum and correlates these oscillations with closed classical orbits. The cylindrical symmetry of the Hamiltonian produces some interesting effects. In particular, at boundary energies the semiclassical approximation fails as a focused cusp approaches the origin. [S1050-2947(97)03306-4]

PACS number(s): 32.80.Gc

I. INTRODUCTION

Experimental measurements of the photodetachment cross section of H⁻ in strong static electric fields were made by Bryant *et al.* [1]. For energies above the threshold energy the resulting cross section was found to be a smooth background upon which was superposed sinusoidal oscillations. Theoretical discussions of the measurements have been given by a number of authors [2,3]. The oscillations arise as an interference effect because the outgoing electron can move against the electric force and then return to the atom. It was shown in Ref. [3] that the cross section could be expressed in the following way:

$$\sigma(E) = \sigma_0(E) + C(E)\sin\Phi(E),$$

where σ_0 is the cross section in the absence of any external fields and $C(E)$ and $\Phi(E)$ are called the recurrence strength and recurrence phase associated with the returning orbit.

Theoretical calculations [4,5] show that analogous oscillations occur for photodetachment in crossed electric and magnetic fields, and that the oscillations are again associated with closed orbits. Quantum calculations have shown that very strong oscillations are present in parallel fields [6], but the relationship to closed orbits was not made clear. Our original motivation in the present paper was to complete this subject by calculating the closed orbits and the resulting spectral oscillations for photodetachment of an electron from H⁻ in parallel electric and magnetic fields. This is a system in which the recurrences are simple, strong, relatively easy to observe, and easy to understand.

We found results which go far beyond this topic, and which are connected with many other problems of current interest. We know from study of nonlinear dynamics that even when long-time motion is chaotic, short-time motion remains relatively simple and predictable. Periodic orbits play a central role: in Poincaré's words, they offer "the only opening through which we might try to penetrate the fortress (chaos) which has the reputation of being impregnable." This classical statement holds also in quantum mechanics, wherein the periodic-orbit theory of Gutzwiller, Balian and Bloch, and Berry and Tabor [7] provides a general theoretical framework for studying quantum manifestations of classical chaos. Besides producing oscillations in absorption spectra [8], periodic orbits produce scars in wave functions [9], oscillations in the density of states [10], and real-time recurrences that have been observed in many atoms and molecules [11]. [Similar phenomena are observed in microwaves in cavities [12(a)], in microjunctions [12(b)], and they are calculated to be consequences of certain models in nuclear physics [12(c)].]

Bifurcations of periodic orbits are of particular interest. A bifurcation is defined as the creation of new periodic orbits as a fixed parameter of the system is varied (such as the total energy or the magnetic field strength). New periodic orbits may be created as a stable-unstable pair, or they may split out of a periodic orbit that is already present in the system. Bifurcations are readily observable because they create new recurrences in absorption spectra. Very detailed studies of bifurcations of closed orbits of electrons in atoms in static electric and/or magnetic fields are given in Refs. [13–16].

Partly stimulated by these observations, the mathematical theory of bifurcations of periodic orbits in Hamiltonian systems is moving forward again. There is a huge literature on bifurcation theory, but only a tiny part of that literature deals with the particular structures of bifurcations of periodic orbits in Hamiltonian systems [17]. Meyer [18] showed that such bifurcations typically fall into one of five characteristic patterns, and later, each of these patterns was seen in the diamagnetic Kepler system. Two different characteristic sequences of bifurcations have been identified. Conservative systems are known to have their own type of period-doubling sequence; perhaps more important, a different sequence of bifurcations was predicted and partially described mathematically by Churchill, Pecelli, and Rod [19], and calculated and observed by Main *et al.* [20,14].

Much more remains to be learned. Bifurcations under variation of more than one parameter are being studied, the effects of symmetries and symmetry breaking are being examined, and the behavior of systems with three or more degrees of freedom is under scrutiny.

At a bifurcation, observed recurrences are especially

strong. In fact, semiclassical theory predicts that the recurrence amplitude diverges at every bifurcation, because a bifurcation is correlated with a focus of classical orbits. We have seen many such cases in atomic spectra. This is a deep problem for periodic-orbit theory, because every stable periodic orbit produces such focusing effects, which in turn lead to vanishing denominators in the periodic-orbit sum. An *ad hoc* repair was suggested by Gutzwiller [21], and further examination of the problem was given in [22]. However, there remains a need for a general theory to repair divergences in recurrence spectra caused by bifurcations of closed orbits. In this set of papers we develop such a theory for two cases.

Electron detachment from a negative ion in the presence of static parallel electric and magnetic fields is a key model which opens the door to the solution of these problems. This model has the following properties. (1) It is exactly soluble [23]. (2) It admits a simple structure of closed orbits and their associated recurrences, and it possesses an orderly sequence of bifurcations. (3) At each bifurcation a certain geometrical structure, a cylindrically focused cusp, passes through the origin. This causes the semiclassical approximation to fail. (4) The failure is repaired by a simple diffraction function, a Fresnel integral. The integral provides a uniform approximation which is always finite and which behaves correctly in all the known limits. (5) The focused cusp is sufficiently similar to the structures found in excitation of neutral atoms that it guided us in the derivation of appropriate formulas for those more difficult cases [24(a)]. (6) Finally, the model accurately represents a system on which experimental measurements can test the predictions.

A brief summary of this work was presented already [24(b)], and here we give the details of the theory. We divide our presentation into two parts. In this paper we give the semiclassical treatment. The general relationship between the closed orbits and the photodetachment cross section is given, the closed orbits are described, and the photodetachment cross section is shown, divergences included. In the following paper [25(a)] we analyze the focused cusp and derive an integral representation of the wave function near the cusp. This uniform wave function gives a corrected formula for the photodetachment cross section. We compare that formula with exact quantum calculations [25(a)], and find good agreement. Experimental measurements on this system are not yet available.

On the other hand, experimental measurements on excitations of neutral atoms in electric fields are available, and recurrences associated with bifurcations of closed orbits have been measured. Calculations show that similar cusp structures arise in such systems. We expect therefore that a similar treatment may give a quantitative description of those recurrences. An important difference arises, however: for excitation of neutral atoms we have to take account of the effect of the Coulomb field on the outer electron. The problem is addressed in the third paper [25(b)]. We find good agreement between theory and measurements.

II. THE PHOTODETACHMENT CROSS SECTION

In this section we will closely follow the arguments presented in the paper by Peters and Delos [5], who studied photodetachment of H^- in crossed electric and magnetic fields. The active electron is initially loosely bound to the hydrogen atom by a short-range, spherically symmetric potential. The Hamiltonian governing this electron is

$$H = \frac{1}{2m}\left(p_p^2 + \frac{L_z^2}{\rho^2}\right) + \omega_L L_Z + \frac{1}{2}m\omega_L^2\rho^2 + \frac{1}{2m}p_z^2 + eF_0 z$$
$$+ V_b(r), \qquad (2.1a)$$

where e is the absolute value of the electron charge, ω_L is the Larmor frequency

$$\omega_L = \frac{eH_0}{2mc}, \qquad (2.1b)$$

F_0 and H_0 are the applied electric and magnetic field strengths, $V_b(r)$ is the effective atomic potential energy that binds the active electron to the hydrogen atom, and $L_z = (xp_y - yp_x)$ is the z component of the angular momentum. Since its conjugate variable, the azimuthal angle ϕ, is an ignorable coordinate, L_z is a constant of the motion, which we take to be zero.

The binding energy of the electron is $E_b = \hbar^2 k_b^2/2m$, where E_b is approximately 0.754 eV and the mass of the electron is denoted by m. The valence electron absorbs a photon of energy $E_p = E_b + E$ and its quantum wave propagates outward in all directions. Within the atomic region the electron moves on a straight line at constant speed. As it enters the external region the trajectories "feel" the effects of the imposed electric and magnetic fields and the semiclassical wave is distorted. The photodetachment cross section is proportional to an oscillator-strength density $Df(E)$ and is given by

$$\sigma = \frac{2\pi^2}{mc}e^2\hbar Df(E). \qquad (2.2a)$$

It has been shown that the oscillator-strength density can be put in the form

$$Df(E) = -\frac{2mE_p}{\pi\hbar^2}\,\mathrm{Im}\langle D\Psi_i|\hat{G}^{(+)}|D\Psi_i\rangle. \qquad (2.2b)$$

The outgoing free-particle Green's function is denoted by $\hat{G}^{(+)}$. The dipole operator D is equal to the projection of the electron coordinate onto the direction of polarization of the laser field.

Equation (2.2) can be interpreted in the following way. The initial state is modified by the laser field to give the source function $|D\Psi_i\rangle$. The outgoing Green's function propagates these waves outward at a fixed energy. Asymptotically the outgoing wave is proportional to e^{ikr}/kr. At $5a_0 - 10a_0$ this asymptotic quantum wave is joined to a semiclassical wave. The semiclassical wave is constructed from classical trajectories which propagate through the external region. The trajectories are eventually turned around by the parallel electric and magnetic fields and some are returned to the origin. At around $10a_0$ the returning semiclassical wave

is very nearly a cylindrical plane wave, so we join it to a quantum-mechanical cylindrical plane wave: $J_0(k_\rho\rho)\exp(ik_zz)$. This cylindrical wave is expanded in spherical partial waves and this expansion is used to calculate the overlap with the source function $\langle D\Psi_i|$. Of all the possible classical trajectories it will only be the returning orbits which form any substantial overlap with the initial state.

We show in Appendix A that Eq. (2.2) can be reduced to a very simple formula, which relates the photodetachment cross section to closed orbits of the electron: the photodetachment cross section is given by the formula

$$\sigma = \sigma_0 + \sum_j \ C_j(E)\sin\Phi_j(E). \qquad (2.3)$$

σ_0 is the photodetachment cross section in the absence of fields. The other terms are oscillatory contributions arising from the returning orbits (the recurrences). The summation is over all closed orbits that begin and end at the nucleus. The phase $\Phi_j(E)$ of the oscillations is given by

$$\Phi_j(E) = -S_j(E)/\hbar + \phi_j + \mu_j \ \frac{\pi}{2}. \qquad (2.4)$$

$S_j(E)$ is the classical action for the returning orbit evaluated at its return time. The returning orbit passes through caustics and foci on its way back to the origin and at each such ''singular point'' the phase undergoes a change of $\pi/2$. The Maslov index μ_j is equal to the total number of singular points (including their multiplicity) through which the electron passes on its journey. The semiclassical wave and its trajectories return to a spherical surface located ar $r=r_{\rm ret}$ a few bohrs from the origin. The Maslov index is calculated along the trajectory that ends at this surface. The semiclassical wave is joined to a quantum wave which is then propagated in to the origin. For parallel fields this wave is a cylindrical plane wave with a focus at the origin. This focus gives rise to an additional phase shift given by ϕ_j. The action, Maslov index, and phase will be found to be independent of the polarization.

The coefficients $C_j(E)$, or the *recurrence amplitudes*, are given by

$$C_j(E) = \sigma_0 6|\chi(\theta_j)|^2 \frac{|f_{\rm out}^{(+)j}|}{|f_{\rm ret}^{(-)j}|} \frac{|J_j(t_0)|^{1/2}}{|J_j(t_{\rm ret})|^{1/2}}. \qquad (2.5)$$

This formula contains both ''classical'' and ''quantum'' factors. The recurrence amplitudes are proportional to the ''direct'' photodetachment cross section σ_0. $\chi(\theta,\phi)$ is another quantum factor; it represents the angular distribution of outgoing waves. We assume that the initial bound state of the electron is an s state, and that the light is linearly polarized on the z axis; it follows that $\chi(\theta,\phi) = \cos\theta/\sqrt{4\pi}$. The angle θ_j is the initial and final direction of the jth returning orbit. The quantity $|J_j(t_0)/J_j(t_{\rm ret})|^{1/2}$ is related to the classical density of the returning wave. The ratio $[f_{\rm out}^{(+)j}/f_{\rm ret}^{(-)j}]$ is the ratio of outgoing quantum wave to the returning quantum wave on the boundary sphere.

The only important difference between the present development and that given in Ref. [5] arises because of the cylindrical symmetry that exists for parallel fields. In crossed fields, the returning waves are appropriately described by plane waves, whereas for parallel fields, they are cylindrical waves that propagate in to the origin while simultaneously moving down the z axis. These waves are described by Bessel functions, Eq. (A17), and their overlap with the initial state is found from the partial-wave expansion of these cylindrical waves (rather than the partial-wave expansion of a plane wave as in Ref. [5]).

III. THE CLASSICAL MOTION

In this section we discuss the classical quantities which appear in the photodetachment cross section given above. The initial conditions for the electron trajectories follow from the fact that upon detachment the electron emerges from the boundary sphere at $(\theta_{\rm out},\phi_{\rm out})$ moving radially outward with a speed such that $mv^2/2 = E_p - E_b \equiv E$. Outside this boundary sphere, the atomic potential energy $V_b(r)$ can be neglected. The z component of the angular momentum is zero, and the Hamiltonian separates into motion along the z axis and motion in the perpendicular x-y plane. Accordingly the z motion is uniform acceleration, and the motion in ρ and ϕ is circular cyclotron motion. The azimuthal motion in $\phi(t)$ is ignorable:

$$z(t) = -\frac{1}{2} \frac{eF_0}{m} t^2 + \frac{1}{m} \sqrt{2mE}\cos\theta_{\rm out}t,$$

$$\rho(t) = \frac{1}{m\omega_L} \sqrt{2mE}\sin\theta_{\rm out}|\sin\omega_Lt|,$$

$$\phi(t) = \omega_Lt + \phi_{\rm out}. \qquad (3.1)$$

Notice we have expressed the initial momenta p_{z_0} and p_{ρ_0} as functions of the total energy and the polar angle $\theta_{\rm out}$; this polar angle defines the direction of the initial velocity of the electron. The absolute value sign on $|\sin\omega_Lt|$ occurs because ρ can only be positive. (However, we will draw our pictures with ρ both positive and negative.)

The equation of motion for $z(t)$ is the motion of an electron in an electric field. If the initial momentum $p_{z_0} = \sqrt{2mE}\cos\theta_{\rm out}$ is negative, then $z(t)$ is less than zero for all time and consequently there will be no returning orbits. On the other hand, if the initial momentum p_{z_0} is positive the electron initially moves in the positive z direction against the electric field and consequently returning orbits will exist for certain initial conditions. For a given energy the maximum distance reached along the z axis is given by the expression $z_{\rm max} = (E/eF_0)\cos^2\theta_{\rm out}$. (For the electric field strength considered here typical values of $z_{\rm max}$ for $\theta_{\rm out}=0$ are between 1×10^6 and 3×10^7 a.u.) The time at which the electron returns to the x-y plane is easily shown to be

$$t_{\rm ret}^z = \frac{2\sqrt{2mE}}{eF_0} \cos\theta_{\rm out}. \qquad (3.2)$$

The motion in ρ is that of a harmonic oscillator, and represents cyclotron motion in the magnetic field. The period of the motion is the cyclotron time,

$$t_c = \pi/\omega_L = 2\pi/\omega_c. \tag{3.3}$$

The electron returns to the z axis whenever $t = t^\rho_{\text{ret}} = n\pi/\omega_L$, which is equivalent to n cyclotron times. The maximum distance $\rho_{\max}$ is equal to $(\sqrt{2mE}/m\omega_L)\sin\theta_{\text{out}}$. Typical values range from 10^6 to 10^7 atomic units.

We see from the above comments that for returning orbits the initial polar angle θ_{out} and therefore the magnitudes of p_{z_0} and p_{ρ_0}, must be such that when the electron returns to the x-y plane in its $z(t)$ motion it also returns to the z axis in its $\rho(t)$ motion, i.e., $t^z_{\text{ret}} = t^\rho_{\text{ret}}$.

It follows that one returning orbit always exists: it lies on the positive z axis; the electron is affected only by the force of the electric field and this force returns it to the origin. At very low energies this is the only orbit that can exist. The return time for ρ motion is the fixed cyclotron time, independent of the energy and independent of the radius of the motion. However, the return time for z motion cannot exceed

$$t_\parallel(E) = 2(2mE/eF_0)^{1/2}, \tag{3.4}$$

which at small E may be much less than the cyclotron time. Therefore, for energies such that $t_\parallel(E) < \pi/\omega_L$, the only possible returning orbit lies on the positive z axis.

If we increase the electron's energy, the return time of the parallel orbit also increases until, at the first ''bifurcation energy,'' it is exactly equal to one cyclotron time. At this point, a new returning orbit is created. Increasing the energy further, the return time of the parallel orbit continues to increase. However, by ''aiming'' the electron at a different angle, we put less energy into the z motion and more into the ρ motion. Above the first bifurcation energy there always exists an initial direction that divides the energy between the two modes in such a way that the z return time equals the ρ return time, π/ω_L. Thus the orbit goes up and down in z while simultaneously executing a single circle in (x,y).

We may say that the new orbit is created out of the parallel orbit, and it moves away as the energy is increased. This phenomenon is what we define as a *bifurcation of an orbit closed at the origin*.

As we increase the energy further, a second ''bifurcation energy'' occurs, at which the return time of the parallel orbit is exactly twice the cyclotron period. At this point another new returning orbit is created, which undergoes two cyclotron circles in (x,y) while simultaneously moving up and down in z. Increasing the energy still further takes us through a discrete set of bifurcation energies, where at each such energy one new orbit is created. The jth new orbit has a return time equal to j cyclotron times, so at any energy, the total number of returning orbits is equal to the smallest integer greater than $t_\parallel(E)/t_c$ where $t_\parallel(E)$ is the return time of the parallel orbit and t_c is the cyclotron time.

We need to know exactly what happens to the whole family of outgoing trajectories at a bifurcation. In Fig. 1 we show families of trajectories in the (ρ,z) plane for various energies. As stated earlier, each family is defined by the condition that the electron begins at the origin with fixed speed moving in any direction. For low energies we have the family of trajectories depicted in Fig. 1(a). We see from the figure that although the electron is confined in its ρ motion it is ultimately swept away from the region near the origin by the electric field. There is one returning orbit for this energy, the parallel orbit, and its trajectory has been emphasized in the figure.

Caustics, or boundaries between classically allowed and forbidden regions, are apparent. These are known as ''fold caustics''; in the upper part of the figure, the parallel orbit touches a fold at the top of its motion. Caustics are significant because semiclassical approximations diverge at a caustic. The approximations can be repaired locally by certain diffraction integrals (such as Airy functions), and these repairs produce additional phase shifts in semiclassical formulas (the Maslov index was invented to keep track of these phase shifts).

In the lower part of the figure, caustics come together to form an upward-pointing cusp, whose tip is located at $z \approx -2 \times 10^3$ a.u. Since ϕ is an ignorable coordinate this cusp is actually a three-dimensional structure, which we call a focused cusp, obtained by rotating the two-dimensional cusp through 2π. This focused cusp is ''unusual.'' General principles based upon catastrophe theory assert that only certain structures of caustics commonly occur. For a ''typical'' or ''generic'' two-dimensional family of trajectories only two kinds of caustics occur: folds and cusps. In three dimensions other types can be present (swallowtails, butterflies, and elliptic umbilics), but a focused cusp is not on the generic list. The reason is obvious: this focused cusp is present because of the cylindrical symmetry of our system. ''Generic'' systems have no such special symmetries, and therefore do not admit such phenomena. On the other hand, what is nongeneric in mathematics can be very common in physics. Indeed, our motivation for studying this phenomenon arises because we have already found many similar examples in other systems [25(b)]. The present case is the simplest one of its type.

Most important, the focused cusp is directly connected with the bifurcations of the parallel orbit. As we increase the energy this cusp rises towards the origin, and there exists an energy at which the tip of the cusp precisely touches the origin [Fig. 1(b)]. This energy is the first bifurcation energy, where a new closed orbit is created.

In Fig. 1(c) we show the family of trajectories at an energy above the first bifurcation energy but below the second, where $E_{b=1} < E < E_{b=2}$. The new orbit created at the first boundary energy is shown along with the initial parallel orbit. One sees that this new orbit touches a caustic at $\rho_{\max}$ and returns to a focus at the origin. The cusp which was previously located below the x-y plane in Fig. 2 has now risen to a position where its tip is located at approximately $z \approx +3.2 \times 10^3$ a.u. The parallel orbit goes up from the origin, touches the caustic at its highest point, and then passes through this cusp on its way back down. At the caustic, the Maslov index increases by 1, as usual, but at the focused cusp, it increases by 2.

Another cusp at $z \approx -4.2 \times 10^3$ a.u. has appeared. As we increase the energy to the second bifurcation energy $E_{b=2}$ this cusp touches the origin [Fig. 1(d)], and the second new orbit is created.
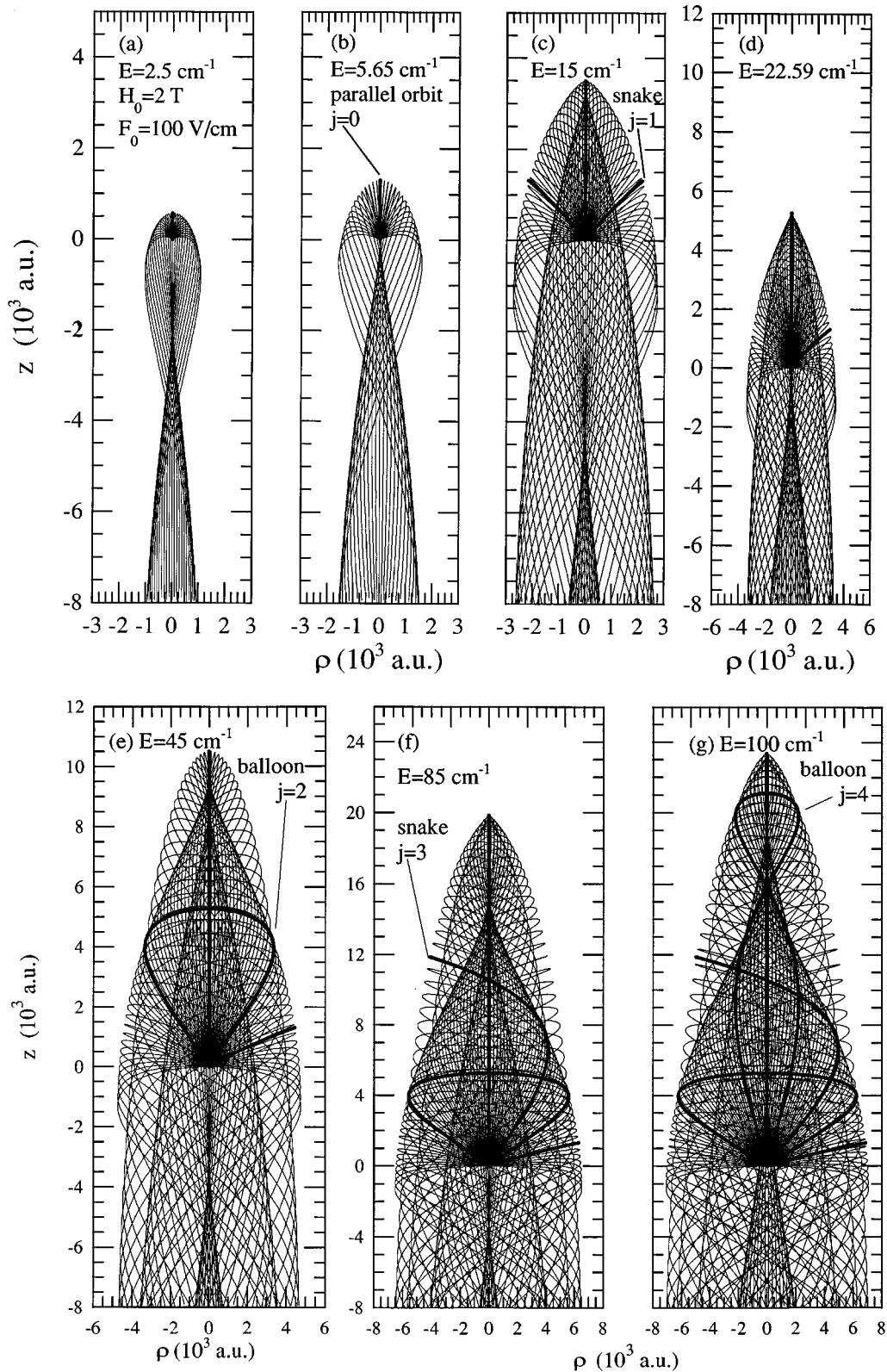
FIG. 1. The family of electron trajectories going out from the origin with fixed speed, and with p_z positive. In every case $H_0 = 2T$ and $F_0 = 100$ V/cm. The trajectories are projected into cylindrical coordinates $[\rho(t), z(t)]$, but they are drawn such that $\rho(t)$ alternates positive and negative [the absolute value in Eq. (3.1) is omitted]. The units are 10^3 bohrs. Note the changes of scale at (d) and (f). (a) At low energies, only the parallel orbit returns to the origin. (b) At the first bifurcation energy a cusp touches the origin and the neighbors of the parallel orbit also return very close to the origin. (c) The first "snake" ($j=1$) has bifurcated out of the parallel orbit, and another cusp is approaching the origin from below. (d) At the second bifurcation energy that cusp touches the origin and (e) the "balloon" ($j=2$) appears. (f) Above the third bifurcation energy another snake ($j=3$) has been created and (g) above the fourth is the double balloon ($j=4$).
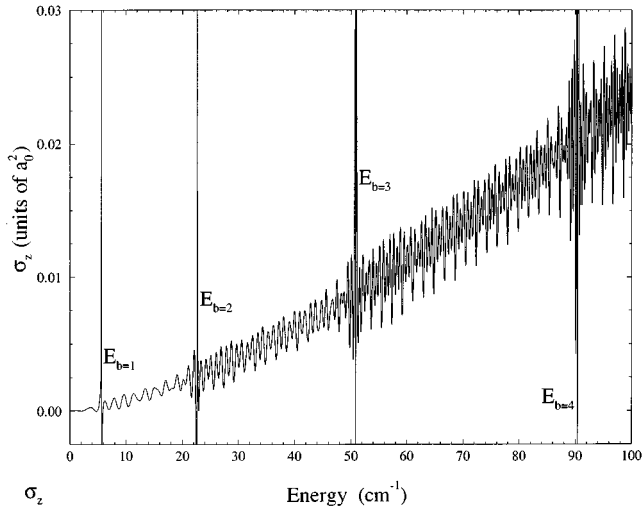
FIG. 2. Semiclassical calculation of photoabsorption cross section near the detachment threshold in parallel fields $F_0 = 100$ V/cm, $H_0 = 2T$. The cross section has oscillations superposed on a smoothly rising background. In the semiclassical calculation each bifurcation is strongly marked by a diverging cross section. Cross section is in units of bohrs², energy is in units of cm⁻¹.

Increasing the energy beyond $E_{b=2} \approx 22.59$ cm⁻¹ the second cusp moves upward through the origin and in Fig. 1(e) we see that there are now two cusps on the positive z axis and one cusp in the lower plane. All three returning orbits are depicted, including the one new orbit, which is the symmetric balloon-shaped orbit. Along this trajectory the electron leaves the origin and reflects off the caustic on the right, passes through a focus at the z axis, and, reflecting off the left caustic, returns to the origin. Each of the two caustics and the focus contribute 1 to the Maslov index.

The "snake" orbit has grown longer in length, but still touches only one caustic. The parallel orbit, on the other hand, now passes through two cusps, one on its outward journey, and one on the returning journey; as before, each cusp contributes two and the caustic at the top contributes one to the Maslov index.

As we increase the energy above the energy above the third boundary energy $E_{b=3}$ [Fig. 1(f)] we find three cusps located on the positive z axis and one more new orbit. This new orbit is another "snake" orbit, and it touches caustics or foci five times before returning to the origin. Increasing the energy beyond the fourth boundary energy $E_{b=4}$ we see the creation of the second "balloon" orbit [Fig. 1(g)]. It passes through two more caustics and two more foci than the first balloon orbit. At this high energy the parallel orbit in Fig. 1(g) now touches four focused cusps and one caustic.

In summary, (1) at the lowest energies, there is one and only one orbit that returns to the origin, the parallel orbit, and as the energy is increased there is a sequence of boundary energies at which new orbits bifurcate from it. (2) The nth boundary energy occurs when the return time of the parallel orbit equals n cyclotron times. (3) Between the nth and $(n+1)$st bifurcation energies there are n off-axis closed orbits labeled by an index $j = 1, \dots, n$. In (ρ, z) coordinates they have the shape of "snakes" for j odd and "balloons" for j even. (4) At the bifurcation a focused cusp passes through

the origin. In the immediate vicinity of this cusp, the semiclassical approximation for the wave function diverges, and has to be repaired. (5) At the bifurcation, the Maslov index of the parallel orbit increases by 2; the Maslov index of the newly created orbit equals the Maslov index of the parallel orbit just before the bifurcation. Therefore above the nth bifurcation the Maslov index of the parallel orbit is $(2n+1)$. That for the jth of off-axis orbit is always $(2j-1)$.

Further details and the analytic description of the phenomena discussed above are given in Appendix B.

IV. THE PHOTODETACHMENT CROSS SECTION

Now we combine the results of the preceding sections to obtain the photodetachment cross section in parallel fields. We recall from Sec. II that the photodetachment cross section is given by Eqs. (2.3)–(2.5); it is the no-field cross section plus a sum of oscillatory terms. Each oscillatory term arises from a closed orbit. The closed orbits were described in Sec. III. However, we also need several more pieces of information for Eqs. (2.4) and (2.5): the classical density (ratio of Jacobians) associated with each closed orbit, the polar angle θ_j for each orbit, the ratio of outgoing to returning waves, the classical action, and the additional phase ϕ_j. These are derived in Appendix B, and combined into the final formula for the cross section.

Let us collect the relevant quantities that will appear in the answer. They are the Larmor frequency [Eq. (2.1b)], the return time on the parallel orbit,

$$t_\parallel(E; F_0) = 2(2mE)^{1/2}/eF_0, \quad (4.1)$$

the label of each returning orbit, j, as indicated in Fig. 1; the maximum number of returning orbits b (besides the parallel orbit), given in Eq. (B8); the polar angle for each returning orbit [Eq. (B7)], the action integral for each returning orbit [Eq. (B26b)],

$$S_j(E; F_0, H_0) = \frac{(2mE)^{1/2}}{meF_0} \cos\theta_j (1 - \tfrac{1}{3}\cos^2\theta_j), \quad (4.2)$$

the "direct" detachment cross section in the absence of fields, $\sigma_{dir} = \sigma_0$, given in Eq. (A10); and one more quantity,

$$N(E; H_0) = E/2\hbar\omega_L = E/\hbar\omega_C, \quad (4.3)$$

which is equal to the energy of the detached electron divided by the spacing between Landau levels, or approximately the number of Landau levels that can be exited at the given energy.

In terms of these quantities, the oscillatory part of the photodetachment cross section for linear z-polarized radiation is

$$\sigma = \sigma_{dir} + \sum_{j=0}^{b} \sigma_{ret}^j, \quad (4.4a)$$

$$\sigma_{ret}^{j=0} = -\sigma_{dir} \frac{3}{4} \left| N(E; H_0) \sin[\omega_L t_\parallel(E; F_0)] \right|^{-1}$$

$$\times \sin[S_{j=0}(E; F_0)/\hbar - \mu_0 \pi/2], \quad (4.4b)$$

$$\sigma_{\text{ret}}^{j \neq 0} = \sigma_{\text{dir}} \frac{3}{\sqrt{2}} \left[N(E;H_0)j \right]^{-1/2} \cos^2 \theta_j$$

$$\times \sin \left(S_j(E;F_0,H_0)/\hbar - \mu_j \frac{\pi}{2} - \frac{\pi}{4} \right). \quad (4.4c)$$

Accordingly, the recurrence amplitudes are

$$C_0 = \tfrac{3}{4} \sigma_{\text{dir}} |N(E,H_0) \sin[\omega_L t_\parallel(E;F_0)]|^{-1}, \quad (4.5a)$$

$$C_{j \neq 0} = \frac{3}{\sqrt{2}} \sigma_{\text{dir}} |N(E,H_0)j|^{-1/2} \cos^2 \theta_j. \quad (4.5b)$$

The quantity $\cos^2 \theta_j$ in Eq. (4.4c) comes from the angular distribution of outgoing waves for z-polarized light. The j in the denominator is related to the intensity of the returning wave associated with the jth orbit. For larger j, the orbits travel longer before returning, and (this being a regular system) on the average the classical density falls off inversely with the time duration of the orbit. The quantity $|\sin \omega_L t_\parallel|^{-1}$ in Eq. (4.4b) comes from the classical density in the vicinity of the parallel orbit. The neighbors of the parallel orbit are oscillating about it with the cyclotron motion of the electron, and they come together in a cusped focus at regular intervals. The quantity $N(E;H_0)$ was explained above; since it appears in the denominator, we may say that the size of the oscillations associated with the parallel orbit is "of order $\hbar$," while those associated with other orbits are "of order $\hbar^{1/2}$."

The extra term $\phi_j = \pi/4$ appearing in the phase of Eq. (4.4c) arises from the fact that the returning quantum wave Eq. (A17) has an additional phase which arises from the asymptotic expansion for the Bessel function. It is connected with the fact that returning waves associated with off-axis orbits are approaching a cylindrical focus. For the parallel orbit, ρ is always zero; we do not use the asymptotic formula for the Bessel function and so we find that $\phi_j = 0$. The returning wave associated with the parallel orbit is (except near the bifurcations) a simple downward-moving plane wave, not a circular wave.

Let us see the consequences of this formula. In Fig. 2 we show the photodetachment cross section calculated from Eq. (4.4). (We used a Sun workstation, but a programmable calculator is sufficient.) The cross section has smoothly rising background with small oscillations. At the lowest energies, the only recurrence is associated with the parallel orbit, so the ripples are small and simple. Each bifurcation energy is clearly marked by a divergence in the semiclassical formula. At energies above each bifurcation, a new closed orbit produces a new set of ripples that beats against all the others.

This is made more clear in Fig. 3, where we show the oscillatory part of the cross section, subtracting the smooth background. The uppermost curve comes from a fully quantum calculation [4,6]. Below it is the complete semiclassical result, and the contribution of each individual orbit. As was found in other cases [5,8,13–16], the semiclassical result is in excellent agreement with the full quantum result at all energies that are not very close to a bifurcation.

A corrected semiclassical approximation that holds near the bifurcations will be given in the following paper [25(a)].
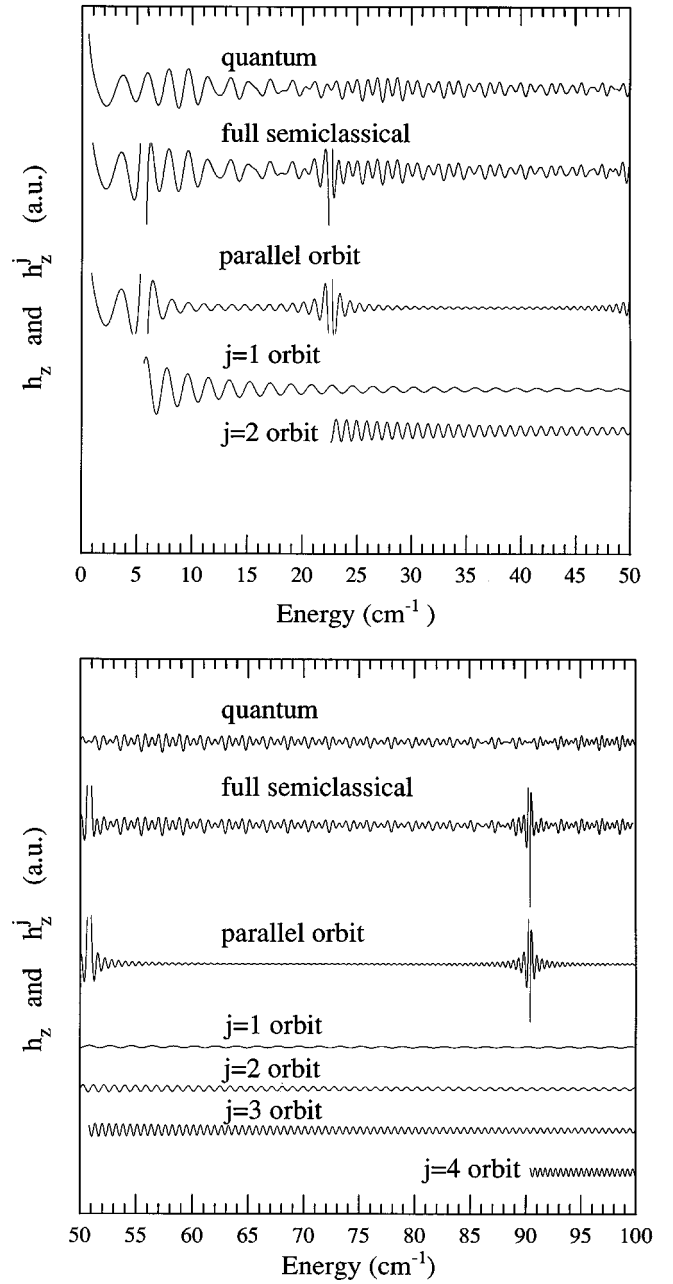

FIG. 3. Oscillatory part of the photoabsorption cross section based on quantum formulas given in Ref. [4]. Oscillatory part of photoabsorption cross section based on semiclassical formulas. Contributions arising from each individual orbit are shown below.

APPENDIX A: DERIVATION OF EQS. (2.3)–(2.5)

1. The initial wave function and dipole operator

We use the following approximation for the initial state of the active electron:

$$\Psi_i(r) = B_0 \frac{e^{-k_b r}}{r} \equiv \frac{1}{\sqrt{4\pi}} R(r). \quad (A1)$$

B_0 is a "normalization" constant [3] and the appropriate value is 0.315 52 in a.u. The constant k_b is related to the binding energy of the active electron $E_b = \hbar^2 k_b^2 2m$.

When the dipole operator $(D = a_x x + a_y y + a_z z)$ acts on the initial state it produces a p wave,

$$|D\Psi_i\rangle = rR(r)\chi(\theta, \phi), \qquad (A2)$$

and we consider only linear z-polarized radiation, so

$$\chi(\theta, \phi) = \chi(\theta) = \frac{1}{\sqrt{4\pi}} \cos\theta. \qquad (A3)$$

2. The Green function, outgoing waves, and the direct contribution to the cross section

In the photodetachment process we may say that the laser prepares a "source function" $|D\Psi_i\rangle$ the detached electron [see Eqs. (2.2b) and (A2)]. The Green function $\hat{G}^{(+)}(\mathbf{q}, \mathbf{q}'; E)$ propagates the electron from the source point at $\mathbf{q}'$ to the field point at $\mathbf{q}$. Since the initial state is localized in coordinate space, the relevant source points and field points all lie within a few bohrs of the nucleus, i.e., within the atomic region.

The Green function propagates the disturbance from the source point at $\mathbf{q}'$ to the field point at $\mathbf{q}$ along two or more paths. The first path is associated with waves which propagate from $\mathbf{q}'$ to $\mathbf{q}$ without ever leaving the atomic region. We refer to this as the direct path. Additionally, there are waves which propagate outward from the source point at $\mathbf{q}'$ and enter the external region where they interact with the laboratory fields. The electric and magnetic fields turn these waves around and some return to the vicinity of the nucleus where they arrive at the field point $\mathbf{q}$. We refer to these as returning paths. With this in mind we write the Green function in the following way:

$$\hat{G}^{(+)}(\mathbf{q}, \mathbf{q}'; E) = \hat{G}_{\text{dir}}^{(+)}(\mathbf{q}, \mathbf{q}'; E) + \hat{G}_{\text{ret}}^{(+)}(\mathbf{q}, \mathbf{q}'; E). \qquad (A4)$$

From Eq. (2.2) it follows that the cross section can be separated in a similar manner, i.e., $\sigma = \sigma_{\text{dir}} + \sigma_{\text{ret}}$.

Since the atomic potential has a short range the waves quickly propagate outside the influence of the atom and through a region $(3a_0 \leq r \leq 100a_0)$ where neither the atomic potential nor the applied fields have any significant effect. We conclude that the appropriate Green function which propagates these waves is the free-particle Green function given by

$$G^{(+)} = \sum_{\ell, m} g_\ell^E(r, r') Y_{\ell, m}(\theta, \phi) Y_{\ell, m}^*(\theta', \phi'), \qquad (A5)$$

where

$$g_\ell^E(r, r') = \left[\frac{-2im}{\hbar^2} \right] k j_\ell(kr_<) h_\ell^{(+)}(kr_>). \qquad (A6)$$

We define the radial dipole integral

$$I_\ell(k) \equiv \int_0^\infty j_\ell(kr') r'^3 R(r') dr' \qquad (A7)$$

and for $\ell = 1$ we have [3,5]

$$I_{\ell=1}(k) = B_0 \sqrt{4\pi} \frac{2k}{(k_b^2 + k^2)^2}. \qquad (A8)$$

The outgoing wave can now be evaluated and we find it to be equal to

$$\hat{G}^{(+)}|D\Psi_i\rangle = \frac{-2im}{\hbar^2} k h_{\ell=1}^{(+)}(kr) I_{\ell=1}(k)\chi(\theta). \qquad (A9)$$

The amplitude of this outgoing wave is proportional to the radial dipole integral, and its angular distribution is given by the function $\chi(\theta)$.

With these results it is possible to evaluate the direct contribution to the photodetachment cross section:

$$\sigma_{\text{dir}} = \sigma_0 = \frac{8\pi m e^2 E_p}{3\hbar^3 c} k I_1^2(k) \qquad (A10a)$$

$$= \frac{64\pi^2 e^2}{3\hbar c} B_0^2 \frac{k^3}{(k_b^2 + k^2)^3}. \qquad (A10b)$$

σ_0 is the no-field cross section: Since the external fields only affect the large scale motion of the electron (motion in the external region) the direct contribution to the cross section is the same as if there were no fields present.

3. Returning waves and spectral oscillations

a. The direct part produces an outgoing wave

Equation (A9) gave an expression for this outgoing wave, and at fairly large distances the asymptotic form of the Hankel function can be used to obtain

$$\hat{G}_{\text{dir}}^{(+)}|D\Psi_i\rangle \approx \frac{2im}{\hbar^2} k I_{\ell=1}(k)\chi(\theta) f_{\text{out}}^{(+)}(kr), \qquad (A11)$$

where we have defined the quantity

$$f_{\text{out}}^{(+)}(kr) \equiv \frac{e^{ikr}}{kr}. \qquad (A12)$$

b. The outgoing wave is joined to a semiclassical wave, which propagates to large distances

To construct the semiclassical wave function we start from a spherical surface centered at the origin with radius $r_{\text{out}} \approx 10a_0$. The spherical angles θ_{out} and ϕ_{out} are chosen as two coordinates spanning this initial surface ($\mathbf{q}^0$). If the outgoing wave evaluated on this surface is written as

$$\Psi(\mathbf{q}^0) = (\hat{G}^{(+)}|D\Psi_i\rangle)_{r = r_{\text{out}}} \qquad (A13)$$

then the semiclassical approximation to the wave $\Psi(\mathbf{q})$ outside this surface is given by

$$\Psi(\mathbf{q}) = \sum_j \Psi(\mathbf{q}^0) A_j(\mathbf{q}) e^{i[S_j(q)/\hbar - \mu_j \pi/2]}, \qquad (A14)$$

where

$$S_j(\mathbf{q}) = \int_{q_0}^q \mathbf{p}\, d\mathbf{q}, \qquad (A15)$$

$$A_j(\mathbf{q}) = \left[\frac{J(t=0, \mathbf{q}_j^0)}{J(t, \mathbf{q}_j^0)}\right]^{1/2},$$

$$J(t, \mathbf{q}_j^0) = \det\left[\frac{\partial \mathbf{q}(t, \mathbf{q}_j^0)}{\partial(t, \mathbf{q}_j^0)}\right].$$

The classical action is given by $S_j(\mathbf{q})$, the Jacobian $J(t, \mathbf{q}_j^0)$ measures the divergence of adjacent trajectories from a central trajectory, and μ_j is the Maslov index. The summation is over all trajectories which arrive at the point $\mathbf{q}$ from different points $\mathbf{q}^0$ on the initial surface.

c. The semiclassical wave returns

As the trajectories are turned around by the electric and magnetic fields, Eq. (A14), describes their associated wave function. Certain of the orbits return to the initial sphere, and there is a discrete set of trajectories that return exactly to the origin. Each such closed orbit passes through the initial sphere with coordinates $\{r_{\text{ret}}, \theta_{\text{ret}}^j, \phi_{\text{ret}}^j\}$ and the kinetic momentum of the returning electron at that point is $m\vec{v}_{\text{ret}}^j \equiv \hbar \vec{k}_{\text{ret}}$. Around each such closed orbit, or central trajectory, there is a family of trajectories which also returns to the sphere. These trajectories stay close to the central trajectory and the ratio of Jacobians measures the classical density associated with this family of trajectories.

The returning wave function associated with each returning family evaluated on the sphere defined by r_{ret} is therefore given by Eqs. (A11)–(A14).

$$\Psi_{\text{ret}}^j(r_{\text{ret}}, \theta_{\text{ret}}, \phi_{\text{ret}}) = \left[\frac{2im}{\hbar^2} kI_{\ell=1}(k)\chi(\theta_{\text{out}}^j)f_{\text{out}}^{(+)}(kr_{\text{out}})\right]$$
$$\times \left|\frac{J_j(t_0)}{J_j(t_{\text{ret}})}\right|^{1/2} e^{i[S_j(t_{\text{ret}})/\hbar - \mu_j\pi/2]}. \quad (A16)$$

Inside the sphere, the external fields can be neglected, and the waves are approximately free waves of the appropriate symmetry. [We can still neglect $V_b(r)$ for $r > 1a_0$.]

In our earlier study of perpendicular electric and magnetic fields, the returning quantum wave was approximated by a plane wave. For parallel electric and magnetic fields, on the other hand, the returning wave near the origin must be cylindrically symmetric, and so will be approximated by a Bessel function. In this case then

$$f_{\text{ret}}(\rho, z) \approx \frac{1}{\sqrt{2\pi}} J_0(k_\rho^{\text{ret}}\rho) \frac{1}{\sqrt{2\pi}} e^{ik_z^{\text{ret}}z}. \quad (A17)$$

At moderate distances, the Bessel function can be separated into incoming and outgoing parts, and the incoming part of $f_{\text{ret}}(\rho, z)$ must match the semiclassical returning wave (A16):

$$\Psi_{\text{ret}}^j(r) \approx N_j f_{\text{ret}}^{(-)j}(\rho, z). \quad (A18)$$

The normalization factor N_j can be determined by letting $r \to r_{\text{ret}}$ and combining Eqs. (A16)–(A18),

$$N_j = \left[\frac{2im}{\hbar^2} kI_{\ell=1}(k)\chi(\theta_{\text{out}}^j)\right]\left|\frac{f_{\text{out}}^{(+)j}}{f_{\text{ret}}^{(-)j}}\right|\left|\frac{J_j(t_0)}{J_j(t_{\text{ret}})}\right|^{1/2}$$
$$\times \exp[iS_j/\hbar - \phi_j - \mu_j\pi/2]. \quad (A19)$$

$S_j(E)$ is the action integral evaluated over the full closed orbit starting and ending at the origin. We have placed an absolute value on the ratio $f_{\text{out}}^{+j}/f_{\text{ret}}^{-j}$, and put its relevant phase into $\exp(-i\phi_j)$. If the approximations we have made are valid then N_j will be independent of the radius of the final sphere r_{ret}. We will find this to be the case, and in particular when we take the limit that $r_{\text{out}} = r_{\text{ret}} \to 0$ the product of the two ratios

$$\mathfrak{R}_j = \left|\frac{f_{\text{out}}^{(+)j}}{f_{\text{ret}}^{(-)j}}\right|\left|\frac{J_j(t_0)}{J_j(t_{\text{ret}})}\right|^{1/2} \qquad (A20)$$

approaches a finite value. This limit will have to be evaluated separately for the parallel orbit and for the off-axis orbits. It will be evaluated in Appendix B 4.

d. The returning wave overlaps the initial state

The expansion of the cylindrical plane wave, Eq. (A17), in spherical harmonics can be obtained from Greene [26] and is given by

$$\Psi_{\text{ret}}^j(r) = N_j \sum_\ell 2i^\ell j_\ell(kr)Y_{\ell,m=0}(\theta, \phi)Y_{\ell,m=0}^*(\theta_{k_{\text{ret}}^j}, \phi_{k_{\text{ret}}^j}), \qquad (A21)$$

where $\{\theta_{k_{\text{ret}}^j}, \phi_{k_{\text{ret}}^j}\}$ are angles defining the direction of k_{ret}^j, the direction in which the returning wave is propagating. We would like to express this in terms of the angles θ_{ret} and ϕ_{ret} or the direction from which the returning trajectory comes. Since $\theta_{\text{ret}} = \pi - \theta_{k_{\text{ret}}^j}$ and $\phi_{\text{ret}} = \pi + \phi_{k_{\text{ret}}^j}$,

$$\Psi_{\text{ret}}^j(r) = N_j \sum_\ell 2(-i)^\ell j_\ell(kr)Y_{\ell,m=0}(\theta, \phi)$$
$$\times Y_{\ell,m=0}^*(\theta_{\text{ret}}^j, \phi_{\text{ret}}^j). \qquad (A22)$$

The oscillatory contribution to the cross section (σ_{ret}) can now be calculated by evaluating the overlap of the returning wave with the function $\langle D\Psi_i|$, and taking the imaginary part,

$$\sigma_{\text{ret}} = \frac{8\pi e^2 2mE_p}{c\hbar^3} kI_{\ell=1}^2 \sum_j |\mathfrak{R}_j|\chi(\theta_{\text{out}}^j)\chi^*(\theta_{\text{ret}}^j)\sin\Phi_j$$

$$= \sigma_0 6 \sum_j |\mathfrak{R}_j|\chi(\theta_{\text{out}}^j)\chi^*(\theta_{\text{ret}}^j)\sin\Phi_j, \qquad (A23)$$

where

$$\Phi_j = -S_j/\hbar + \phi_j + \mu_j\pi/2.$$

We have arrived at Eqs. (2.3)–(2.5).

APPENDIX B:
RETURNING ORBITS—QUANTITATIVE THEORY

Here we give a quantitative analysis of the returning orbits. In particular, we will derive: (i) A formula for the boundary energies at which the new orbits appear. (ii) A formula for the Jacobian which gives the classical density associated with the trajectories and therefore the amplitude of the returning wave. We will also verify our observations concerning the number of singular points along a trajectory, and will calculate the Maslov index for the two classes of trajectories. (iii) A formula for the classical action on an orbit. This determines the phase of the returning wave.

1. Hamiltonian equations of motion

Starting from our Hamiltonian in cylindrical coordinates, with $L_z = 0$, [Eq. (3.1)], we can eliminate unnecessary parameters by using the scale change

$$q' = m \frac{\omega_L^2}{eF_0} q, \tag{B1a}$$

$$p' = \frac{\omega_L}{eF_0} p, \tag{B1b}$$

$$H' = \left[\frac{1}{m} \left(\frac{eF_0}{\omega_L} \right)^2 \right]^{-1} H, \tag{B1c}$$

$$t' = \omega_L t, \tag{B1d}$$

which gives

$$H = \tfrac{1}{2} p_\rho^2 + \tfrac{1}{2} \rho^2 + \tfrac{1}{2} p_z^2 + z, \tag{B2}$$

where we have dropped the primes and all variables are now in dimensionless form.

As stated previously, the initial speed is a constant and the initial direction is given by the polar angle θ_{out}. The initial momentum is proportional to this velocity, i.e., $p_\rho(t) = d\rho(t)/dt$ and $p_z(t) = dz(t)/dt$. With this in mind we rewrite Eqs. (3.1) in their dimensionless form,

$$z(t) = -\frac{1}{2} t^2 + \sqrt{2E} \cos\theta_{out} t,$$
$$\tag{B3}$$
$$\rho(t) = \sqrt{2E} \sin\theta_{out} \sin t.$$

We can also relate the polar angle θ_{out} to the initial energy and momenta by

$$\sin\theta_{out} = \frac{p_{\rho 0}}{\sqrt{2E}}, $$

$$\cos\theta_{out} = \frac{p_{z0}}{\sqrt{2E}}. \tag{B4}$$

2. Initial conditions for closed orbits and the boundary orbits

In this section we will give quantitative conditions for returning orbits, determine how many closed orbits exist at each energy, and determine the bifurcation energies where new orbits are created.

From Eq. (B3) there can be no returning orbits for $\theta_{out} \geq \pi/2$. Looking at Eq. (B3) we see that the time for the electron to return to the x-y plane ($z=0$) is given by

$$t_{ret}^z = 2\sqrt{2E} \cos\theta_{out} \rightarrow \frac{2\sqrt{2mE}}{eF_0} \cos\theta_{out}. \tag{B5}$$

Here and below formulas after the arrow are in real units (unscaled variables). If the angle θ_{out} is equal to zero the trajectory travels along the z axis, $\rho(t) = 0$, and it returns to the origin at the time $t_{ret}^z = 2\sqrt{2E}$ (scaled units). This is the parallel orbit.

Consider now the other orbits that return to the origin. Their z return time must be the same as their ρ return time,

$$t_{ret}^z = t_{ret}^\rho = n\pi \rightarrow n\pi/\omega_L, \tag{B6}$$

so for a given energy E, Eq. (B5) specifies the initial polar angle for a returning orbit,

$$\cos\theta_j \equiv \cos\theta_{out} = \frac{j\pi}{2\sqrt{2E}} \rightarrow \frac{(eF_0/\omega_L) j\pi}{2\sqrt{2mE}} = \frac{j\pi}{\omega_L t_\parallel(E;F_0)}, \tag{B7}$$

where j is a positive integer from 1 to some j_{max}. This maximum integer is given by

$$b \equiv j_{max} = \text{Int}\left[\frac{2\sqrt{2E}}{\pi} \right] \rightarrow \text{Int}\left[\frac{1}{\pi} \frac{2\sqrt{2mE}}{(eF_0/\omega_L)} \right]$$

$$= \text{Int}[\omega_L t_\parallel(E;F_0)/\pi] \tag{B8}$$

and $\text{Int}(\alpha)$ means "the largest integer less than or equal to α." For each given energy there are b off-axis orbits together with the parallel orbit.

What are the bifurcation energies? From Eq. (B8)

$$E_b = \frac{1}{8} (b\pi)^2 \rightarrow \frac{1}{8m} \left[\frac{eF_0}{\omega_L} b\pi \right]^2, \tag{B9}$$

where again b is an integer labeling the bifurcation.

In Fig. 4 we graphically display the results of the preceding two sections. For energies between zero and the first bifurcation energy $E_{b=1} \approx 1.23$ we have one returning orbit, the parallel orbit with $\theta_{out}^{j=0} = 0$ or the vertical axis. As the total energy is increased through $E_{b=1}$ a new orbit separates from the horizontal axis, its initial polar angle increasing towards $\pi/2$ with increasing energy. As the energy increases to approximately 4.94 scaled units the second bifurcation energy $E_{b=2}$ is reached, and another new returning orbit is created out of the parallel orbit.
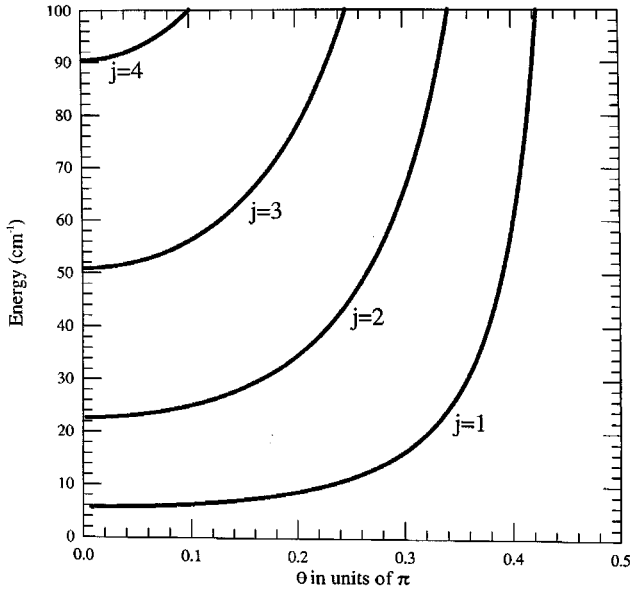
FIG. 4. Initial angle of each bifurcated orbit as a function of energy.

3. The Jacobian

The ratio of Jacobians appears in the semiclassical wave function as an amplitude $A_j(q)$ and represents the divergence of adjacent trajectories in time. As this ratio decreases, the probability density of the wave function is spread out over a larger area. Near the caustics or foci where neighboring trajectories converge to one another the ratio of Jacobians increases, eventually becoming infinite at the singular point. At these points the semiclassical approximation fails.

Here we will calculate the Jacobian by evaluating the expression

$$J(t) = \frac{\partial(x,y,z)}{\partial(t,\theta_{out},\phi_{out})}. \qquad (B10)$$

The coordinates $\{t, \theta_{out}, \phi_{out}\}$ are the coordinates for the family of trajectories, i.e., for the Lagrangian manifold. The intrinsic coordinates of the initial spherical surface centered about the origin with radius r_{out} are $\{\theta_{out}, \phi_{out}\}$, which define the initial direction of motion of the electron. We relate the three-dimensional Jacobian to a two-dimensional Jacobian by

$$J(t,\theta_{out},\phi_{out}) = \rho(t) J_2(t,\theta_{out}), \qquad (B11)$$

where

$$J_2(t,\theta_{out}) = \frac{\partial(z,\rho)}{\partial(t,\theta_{out})}. \qquad (B12)$$

The two-dimensional determinant given in Eq. (B12) is evaluated using the equations of motion [see Eq. (B3)] and the result is

$$J_2(t,\theta_{out}) = 2E \left[\left(\cos\theta_{out} - \frac{1}{\sqrt{2E}} t \right) \sin t \ \cos\theta_{out} \right.$$

$$\left. + t \ \cos t \ \sin^2\theta_{out} \right] \qquad (B13a)$$

or in dimensional form

$$J_2(t,\theta_{out}) = \frac{2E}{m\omega_L} \left[\left(\cos\theta_{out} - \frac{eF_0}{\sqrt{2mE}} t \right) \sin\omega_L t \ \cos\theta_{out} \right.$$

$$\left. + \omega_L t \ \sin^2\theta_{out}\cos\omega_L t \right]. \qquad (B13b)$$

Equation (B13) represents the Jacobian for any trajectory at any arbitrary time, i.e., the trajectory is not necessarily a closed orbit.

The prefactor $\rho(t)$ in Eq. (B11) goes to zero at the beginning and end of any closed orbit, and it is always exactly zero for the parallel orbit. Therefore this quantity must be handled with care. We will obtain the classical density for the parallel orbit by taking the limit as $\theta_{out} \to 0$. The classical density of the other orbits really diverges as $\rho \to 0$, and the semiclassical approximation fails. Therefore the semiclassical wave function must be joined to a Bessel function, which remains finite as $\rho \to 0$.

4. The ratio of Jacobians and $A(q)$

Let us construct the ratio of Jacobians for $t = t_0$ and $t = t_{ret}$. Consider the Jacobian when t_0 is small ($\omega_L t_0 \ll 1$). In this case, expanding the trigonometric functions of Eq. (B13) and keeping only the lowest order, we find

$$J(t_0,\theta_{out}^j) = \rho_0(2E) t_0 = \sqrt{2E} r_0^2 \sin\theta_{out}^j \to (2E/m)^{1/2} r_0^2 \sin\theta_{out}^j, \qquad (B14)$$

where we have used the fact that $t_0 = r_0/v_0$ and v_0 is the initial velocity of the emerging electron.

For the parallel orbit, $\theta_{out}^j = 0$ and $t_{ret} = \sqrt{2E}$. We evaluate J by assuming θ_{out}^j is small but nonzero; then at t_{ret}, Eq. (B13) reduces to

$$J(t_{ret},\theta_{out}^{j=0}) = -(2E)^{3/2}\sin\theta_{out}^{j=0}\sin^2(2\sqrt{2E}). \qquad (B15a)$$

[The factor $\sin\theta_{out}^{j=0}$ will cancel the corresponding factor in Eq. (B14).]

For the other orbits, since $t_{ret} = j\pi$, the Jacobian reduces to

$$J(t_{ret},\theta_{out}^{j \neq 0}) = (-1)^j 2(2E)^{3/2}(\rho_{ret}\sin^2\theta_{out}^j)\cos\theta_{out}^j. \qquad (B15b)$$

The amplitude of the wave function involves the ratio of Jacobians at $t = t_0$ and $t = t_{ret}$. Actually, however, referring back to Eq. (A20), the ratio we need also involves the outgoing and returning quantum waves,

$$|\mathfrak{R}_j| = \left| \frac{f_{out}^{(+)j}}{f_{ret}^{(-)j}} \right| \left| \frac{J_j(t_0)}{J_j(t_{ret})} \right|^{1/2}, \qquad (B16)$$

where the outgoing and returning waves are, respectively, given in Eqs. (A12) and (A17), both of which are to be evaluated on the boundary sphere. This ratio must be considered separately for the parallel orbit or the off-axis orbits.

First we consider the parallel orbit. Since $\rho(t)$ equals zero for all time, the Bessel function in Eq. (B16) should be set equal to one, and the returning quantum wave is approximated by a plane wave directed down the z axis,

$$f_{\text{ret}}^{(-)j=0} = e^{-ikz}/2\pi. \tag{B17}$$

After substituting Eqs. (B15) we have for the limit $r_0 = r_{\text{ret}} \to 0$ of Eq. (B16) that

$$\lim_{r_0, r_{\text{ret}} \to 0} |\mathfrak{R}_{j=0}| = \left(\frac{2\pi}{k}\right) \left|\frac{1}{\sqrt{2E}\sin 2\sqrt{2E}}\right| \tag{B18a}$$

$$\to \left(\frac{2\pi}{k}\right) \left|\frac{\omega_L}{(2E/m)^{1/2}\sin[2\omega_L(2mE)^{1/2}/eF_0]}\right| \tag{B18b}$$

$$\to \frac{2\pi}{k} \frac{\omega_L}{(2E/m)^{1/2}|\sin\omega_L t_\|(E;F_0)|}. \tag{B18c}$$

This expression is finite at all E except when the sin passes through zero. That happens at the bifurcation energies, where the focused cusp touches the origin, and the semiclassical approximation fails. Examining also the phases, we see that for the parallel orbit, $\phi_0 = 0$.

For the off-axis orbits we use the asymptotic approximation to the zero-order Bessel function ($k\rho \gg 1$)

$$J_0(k_\rho \rho) \approx \left(\frac{2}{\pi k_\rho \rho}\right)^{1/2} \cos(k_\rho \rho - \pi/4) \tag{B19}$$

and extract the incoming wave,

$$f_{\text{ret}}^{(-)j} = (2\pi)^{-3/2} (k_\rho \rho)^{-1/2} e^{-ik_\rho \rho} e^{ik_z z} e^{i\pi/4}. \tag{B20}$$

[Here, as in Eqs. (B17) and (B19), we are using the convention that $k_\rho > 0$ and $k_z < 0$, so that this represents a wave approaching the atom from positive ρ and z.]

Using our expressions for the Jacobian of the off-axis orbits evaluated at t_{ret}, and using the fact that $k_\rho = k \sin\theta_{\text{ret}} = k \sin\theta_{\text{out}}$, we find that the ratio (B16) reduces to

$$\lim_{r_0, r_{\text{ret}} \to 0} |\mathfrak{R}_{j \neq 0}| = \frac{2^{3/2}\pi}{k^{1/2}} \left|\frac{\pi}{2\sqrt{2E}\cos\theta_{\text{out}}^j}\right|^{1/2} = \frac{2^{3/2}\pi}{k^{1/2}} j^{-1/2}, \tag{B21}$$

where we have used Eq. (B7) to evaluate $\cos\theta_{\text{out}}^j$. Multiplying numerator and denominator by $\hbar^{1/2}$ and converting back to unscaled units, this quantity becomes

$$\lim_{r_0, r_{\text{ret}} \to 0} |\mathfrak{R}_{j \neq 0}| \to 2\pi \left(\frac{\hbar \omega_L}{E}\right)^{1/2} \frac{1}{j^{1/2}}. \tag{B22}$$

The additional $\pi/4$ in Eqs. (B19) and (B20) implies that $\phi_j = \pi/4$ for all off-axis orbits.

5. The Maslov index

Caustics and foci are singular points where the Jacobian goes to zero and hence the coefficient $A_j(\mathbf{q})$ goes to infinity. Typically, as the electron passes through either a caustic or focus, the Maslov index increases by one. More precisely, however, the Maslov index not only includes the number of singular points along the trajectory but also takes account of the multiplicity of the singular point. For example, if the Jacobian should have a second-order zero, then the Maslov index would increase by two instead of one.

Consider the time dependence of the Jacobian associated with the parallel orbit. From Eqs. (B11) and (B13a) we find that

$$J(t, \theta_{\text{out}}^{j=0}) = (2E)^{3/2} \sin\theta_{\text{out}}^{j=0} \sin^2 t \left[1 - \frac{1}{\sqrt{2E}} t\right]. \tag{B23}$$

The factor $\sin\theta_{\text{out}}^{j=0}$ vanishes in the limit $\theta_{\text{out}} \to 0$, but this cancels. The factor $\sin^2 t$ is a second-order zero at each cusp. Therefore every time the parallel orbit passes through a cusp the Maslov index increases by two. If the energy lies between two bifurcation energies $E_b < E < E_{b+1}$, then $b\pi < t_{\text{ret}} < (b+1)\pi$, so the parallel orbit passes through b cusps on its journey back to the origin. This is the result we obtained earlier by inspection of Fig. 1.

J also vanishes when $t = \sqrt{2E}$, and the term in square brackets in Eq. (B23) is zero. The electron has reached the caustic at the top of its motion. For a given total energy it is clear that the parallel orbit will pass through b second-order cusps and one caustic; the Maslov index is equal to $(2b + 1)$.

We now examine the time dependence of the Jacobian for the off-axis orbits. In this case the zeros of the Jacobian occur whenever the expression

$$J(t, \theta_{\text{out}}^j) = \rho(t) 2E \left[\left(\cos\theta_{\text{out}}^j - \frac{1}{\sqrt{2E}} t\right) \sin t \cos\theta_{\text{out}}^j + t \cos t \sin^2\theta_{\text{out}}^j\right] \tag{B24}$$

is equal to zero. The factor $\rho(t)$ is equal to zero at the cyclotron times so the electron will pass through $(j-1)$ such foci on its journey back to the origin. This does not include the one focus that is at the origin (we always calculate the Maslov index of the returning semiclassical wave before it gets to the origin). The Jacobian also goes to zero at the caustics, when the bracketed expression is equal to zero. After a slight rearrangement we obtain the following transcendental equation for the times t_{cau} at which the electron passes through a caustic:

$$\cot t_{\text{cau}} = \cot^2 \theta_{\text{out}}^j \left[\frac{1}{\sqrt{2E}} \frac{1}{(\cos\theta_{\text{out}}^j)} - \frac{1}{t_{\text{cau}}}\right]. \tag{B25}$$

Examining Eq. (B25) and inspecting Fig. 1 we see that for the off-axis orbits the electron will pass through j caustics. We find therefore that the off-axis returning orbits pass through $(j-1)$ foci and j caustics; the Maslov index is equal to $(2j-1)$. This result is consistent with the pictures in Sec. III.

6. The classical action

The classical action $S(q)$ appears in the phase of the semiclassical wave function and is defined in Eq. (A15). The integrals are evaluated using Eq. (B3) and the expressions for the conjugate momenta in the paragraph following Eq. (B2). The integrals are straightforward and lead to

$$S(t_{\text{ret}}^j, \theta_{\text{out}}^j) = (2E)^{3/2} \cos\theta_{\text{out}}^j \left[1 - \frac{1}{3} \cos^2\theta_{\text{out}}^j \right]. \tag{B26a}$$

This expression is valid for both the parallel orbits and the off-axis orbits. In the dimensional form the classical action is

$$S(t_{\text{ret}}^j, \theta_{\text{out}}^j) = \frac{(2mE)^{3/2}}{meF_0} \cos\theta_{\text{out}}^j \left[1 - \frac{1}{3} \cos^2\theta_{\text{out}}^j \right]. \tag{B26b}$$

7. Returning waves and photodetachment cross section

We combine the results of all the preceding into formulas for the semiclassical returning waves and for the cross sec-

tions. Equations (A18) and (A19) are the returning waves, with appropriate ratios evaluated in Eq. (B18b) or (B22) for the parallel or other orbits, respectively. The resulting wave functions are

$$\Psi_{\text{ret}}^{j=0} = \left(\frac{2im}{\hbar^2} \right) k I_{\ell=1}(k) \chi(\theta_{\text{out}}^0) \exp i\left(S_0/\hbar - \mu_0 \frac{\pi}{2} \right)$$

$$\times \begin{cases} \dfrac{(\omega_L/k)}{(2E/m)^{1/2}|\sin\omega_L t_\parallel(E;F_0)|} \, e^{-ikz} & \text{(B27a)} \\[3mm] \left(\dfrac{\hbar\omega_L}{jE} \right)^{1/2} J_0(k_\rho^j \rho) e^{ik_z^j z}. & \text{(B27b)} \end{cases}$$

The contributions of these returning waves to the cross sections come from Eq. (A23).

$$\sigma_{\text{ret}}^{j=0} = \sigma_0 \frac{12\pi\omega_L/k}{(2E/m)^{1/2}|\sin\omega_L t_\parallel(E;F_0)|} |\chi(\theta=0)|^2$$

$$\times \sin\left(-S_0 + \mu_0 \frac{\pi}{2} \right), \tag{B28a}$$

$$\sigma_{\text{ret}}^{j\neq 0} = \sigma_0 12\pi \left(\frac{\hbar\omega_L}{jE} \right)^{1/2} |\chi(\theta_j)|^2 \sin\left(-S_j + \mu_j \frac{\pi}{2} + \frac{\pi}{4} \right). \tag{B28b}$$

Using $\hbar k = (2mE)^{1/2}$, and using Eq. (A3) for $\chi(\theta)$, we arrive at Eqs. (4.4) and (4.5).

[1] H. C. Bryant, A. Mohagheghi, J. E. Stewart, J. B. Donahue, C. R. Quick, R. A. Reeder, V. Yuan, C. E. Hummer, W. W. Smith, S. Cohen, W. P. Reinhardt, and L. Overman, Phys. Rev. Lett. **58**, 2412 (1987).

[2] I. I. Fabrikant, Zh. Eksp. Teor. Fiz. **79**, 2070 (1980) [Sov. Phys. JETP **52**, 1045 (1980)]; A. R. P. Rau and Hin-Yiu Wong, Phys. Rev. A **37**, 632 (1988); Yu. N. Demkov and G. F. Drukarev, Zh. Eksp. Teor Fiz. **47**, 918 (1964) [Sov. Phys. JETP **20**, 614 (1965)]; W. P. Reinhardt, in *Atomic Excitation and Recombination in External Fields*, edited by M. H. Nayfeh and C. W. Clark (Gordon and Breach, New York, 1985), p. 85; V. Z. Slonim and F. I. Dalidchik, Zh. Eksp. Teor. Fiz. **71**, 2057 (1976) [Sov. Phys. JETP **44**, 1081 (1976)]; H.-Y. Wong, A. R. P. Rau, and C. H. Greene, Phys. Rev. A **37**, 2393 (1988).

[3] M. L. Du and J. B. Delos, Phys. Rev. A **38**, 5609 (1988).

[4] I. I. Fabrikant, Phys. Rev. A **43**, 258 (1991).

[5] A. D. Peters and J. B. Delos, Phys. Rev. A **47**, 3020 (1993); **47**, 3036 (1993).

[6] M. L. Du, Phys. Rev. A **40**, 1330 (1989).

[7] M. Gutzwiller, *Chaos in Classical and Quantum Mechanics* (Springer-Verlag, New York, 1990); R. Balian and C. Bloch, Ann. Phys. (N.Y.) **60**, 401 (1970); **64**, 271 (1971); **69**, 76 (1972); **85**, 514 (1974); M. V. Berry and M. Tabor, Proc. R. Soc. London, Ser. A **349**, 101 (1976).

[8] M. L. Du and J. B. Delos, Phys. Rev. Lett. **58**, 1731 (1987); Phys. Rev. A **38**, 1896 (1988); **38**, 1913 (1988); J. Gao, J. B. Delos, and M. Baruch, *ibid*. **46**, 1449 (1992); J. Gao and J. B.

Delos, *ibid*. **46**, 1455 (1992); E. B. Bogomolnyi, Zh. Eksp. Teor. Fiz. **96**, 487 (1989) [Sov. Phys. JETP **69**, 275 (1989)]; A. Holle, G. Wiebusch, J. Main, B. Hager, H. Rottke, and K. H. Welge, Phys. Rev. Lett. **56**, 2594 (1986); U. Eichmann, K. Richter, D. Wintgen, and W. Sandner, *ibid*. **61**, 2438 (1988); M. Courtney, N. Spellmeyer, H. Jiao, and D. Kleppner, Phys. Rev. A **51**, 3604 (1995).

[9] E. J. Heller, Phys. Rev. Lett. **53**, 1515 (1984).

[10] D. Wintgen, Phys. Rev. Lett. **58**, 1589 (1987); D. Wintgen and H. Friedrich, Phys. Rev. A **36**, 131 (1987).

[11] G. Alber, Phys. Rev. A **40**, 1321 (1989); G. Alber and P. Zoller, Phys. Rep. **199**, 231 (1991); J. A. Yeazell, M. Malla-lieu, and C. R. Stroud, Phys. Rev. Lett. **67**, 2007 (1990); J. A. Yeazell, G. Raithel, L. Marmet, H. Held, and H. Walther, *ibid*. **70**, 2884 (1993); A. ten Wolde, L. D. Noordam, A. Lan-gendijk, and H. B. Linden van den Heuvell, Phys. Rev. A **40**, 485 (1989).

[12] (a) S. Sridhar, Phys. Rev. Lett. **67**, 785 (1991); (b) C. M. Marcus, A. J. Rimberg, R. M. Westervelt, P. F. Hopkins, and A. C. Gossard, *ibid*. **69**, 506 (1992); (c) M. Baranger, M. R. Haggerty, B. Lauritzen, D. C. Meredith, and D. Provost, CHAOS **5**, 261 (1995).

[13] J. M. Mao and J. B. Delos, Phys. Rev. A **45**, 1746 (1992).

[14] J. Main, G. Wiebusch, K. Welge, J. Shaw, and J. B. Delos, Phys. Rev. A **49**, 847 (1994).

[15] J. M. Mao, K. A. Rapelje, S. J. Blodgett-Ford, J. B. Delos, A. König, and H. Rinneberg, Phys. Rev. A **48**, 2117 (1993).

[16] J. Gao and J. B. Delos, Phys. Rev. A **49**, 869 (1994).

[17] H. Poincaré, *New Methods of Celestial Mechanics* (Dover, New York, 1957), Vol. III; G. D. Birkhoff, *Dynamical Systems* (American Mathematical Society, New York, 1926).

[18] K. R. Meyer, Trans. Am. Math. Soc. **149**, 95 (1970); **154**, 273 (1971); K. R. Meyer and G. R. Hall, *Introduction to Hamiltonian Dynamical Systems and the N-Body Problem*, Applied Mathematics Series Vol. 90 (Springer, New York, 1992); M. A. M. de Aguiar, C. P. Malta, M. Baranger, and K. T. R. Davies, Ann. Phys. (N.Y.) **180**, 167 (1987).

[19] R. C. Churchill, G. Pecelli, and D. L. Rod, Arch. Ration. Mech. Anal. **73**, 313 (1980).

[20] J. Main, G. Wiebusch, A. Holle, and K. H. Welge, Phys. Rev. Lett. **57**, 2789 (1986).

[21] M. C. Gutzwiller, J. Math. Phys. (N.Y.) **12**, 343 (1971) [especially the discussion leading to Eq. (37) therein].

[22] M. Beims and G. Alber, Phys. Rev. A **48**, 3123 (1993); M. Kus, F. Haake, and D. Delande, Phys. Rev. Lett. **71**, 2167 (1993); J. Main (private communication).

[23] The simplicity of the model is closely connected with the fact that the time propagator can be written in closed form. A wave-packet theory describing recurrences in real time has been developed by Q. Wang and A. Starace, Phys. Rev. A **51**, 1260 (1995).

[24] (a)M. Courtney, H. Jiao, N. Spellmeyer, D. Kleppner, J. Gao, and J. B. Delos, Phys. Rev. Lett. **74**, 1538 (1995); (b) A. D. Peters, C. Jaffé, and J. B. Delos, *ibid.* **73**, 2825 (1994).

[25] (a)A. D. Peters, C. Jaffé, J. Gao, and J. B. Delos, following paper, Phys. Rev. A **56**, 345 (1997); (b) J. Gao and J. B. Delos, this issue, *ibid.* **56**, 356 (1997).

[26] C. H. Greene, Phys. Rev. A **36**, 4236 (1987).